# Detection of Storm Damage Tracks with EOS Data

GARY J. JEDLOVEC

*National Aeronautics and Space Administration Marshall Space Flight Center, Huntsville, Alabama*

UDAYSANKAR NAIR AND STEPHANIE L. HAINES

*Earth System Science Center, University of Alabama in Huntsville, Huntsville, Alabama*

(Manuscript received 16 December 2004, in final form 8 November 2005)

ABSTRACT

The damage surveys conducted by the NWS in the aftermath of a reported tornadic event are used to document the location of the tornado ground damage track (pathlength and width) and an estimation of the tornado intensity. This study explores the possibility of using near-real-time medium and high spatial resolution satellite imagery from the NASA Earth Observing System satellites to provide additional information for the surveys. Moderate Resolution Imaging Spectroradiometer (MODIS) and Advanced Spaceborne Thermal Emission and Reflection Radiometer (ASTER) data were used to study the damage tracks from three tornadic storms: the La Plata, Maryland, storm of 28 April 2002 and the Ellsinore and Marquand, Missouri, storms of 24 April 2002. These storms varied in intensity and occurred over regions with significantly different land cover. It was found that, depending on the nature of the land cover, tornado damage tracks from intense storms (F1 or greater) and hail storms may be evident in ASTER, Landsat, and MODIS satellite imagery. In areas where the land cover is dominated by forests, the scar patterns can show up very clearly, while in areas of grassland and regions with few trees, scar patterns are not as obvious or cannot be seen at all in the satellite imagery. The detection of previously unidentified segments of a damage track caused by the 24 April 2002 Marquand, Missouri, tornado demonstrates the utility of satellite imagery for damage surveys. However, the capability to detect tornado tracks in satellite imagery depends on the ability to observe the ground without obstruction from space and appears to be as much dependent on the nature of the underlying surface and land cover as on the severity of the tornadic storm.

## 1. Introduction

The continental United States experiences hundreds of tornadic storms every year. On average tornadoes are responsible for $420 million in damage and 70 deaths annually (Brooks and Doswell 2001, 2002). The National Weather Service (NWS), in addition to issuing tornado watches and warnings, is also responsible for conducting surveys of damage caused by tornadic storms. The damage surveys, which include ground and occasionally aerial observations, are used to document the location of the tornado ground track (pathlength and width) and to provide an estimation of the tornado intensity. Damage surveys are conducted soon after the occurrence of a storm and before the storm damage and debris are cleaned up. Ground surveys are time consuming and often fail to identify the entire tornado track or damage region in sparsely populated areas because of limited vehicle access and resources by the local Weather Forecast Office (WFO) staff. Aerial observations are used when available, usually for larger storms and in more populated portions of the country where aerial resources are more readily available.

Multispectral imagery from remote sensing satellites has the potential to provide valuable assistance during damage surveys in the aftermath of severe storm events. Studies have shown that damage caused by severe storm events can be identified in satellite imagery, sometimes for an extended period of time. Ground tracks from tornadoes that occurred in 1965 in eastern Paraguay were found to be still visible on high-resolution Landsat Multispectral Scanner and French Earth Observation Satellite imagery acquired in the 1970s and 1980s (Dyer 1988; Yuan et al. 2002). Bentley

*Corresponding author address:* Dr. Gary Jedlovec, NASA MSFC/XD11, 320 Sparkman Dr., Huntsville, AL 35805.
E-mail: gary.jedlovec@nasa.gov

et al. (2002) used *Landsat-7* Enhanced Thematic Mapper Plus (ETM+) imagery to show the relation between normalized difference vegetation index (NDVI) change and crop damage regions caused by hail and wind in western Illinois. Parker et al. (2005) and Segele et al. (2005) document the use of Moderate Resolution Imaging Spectroradiometer (MODIS) and Advanced Very High Resolution Radiometer (AVHRR) data to detect and delineate areas devegetated by hail and modeled the consequences of such changes on the local atmospheric environment. Yuan et al. (2002) used principal component analysis (PCA) with NDVI imagery derived from Indian Remote Sensing (IRS) satellite data to examine the ground track of the 3 May 1999 Oklahoma City, Oklahoma, tornado. Their results showed that PCA could detect the tornado damage track signatures for F3 and greater regions on the Fujita scale (Fujita 1981, 1987) while the NDVI imagery showed significant spatial correlations with F2 and greater damage regions. In some instances, the NDVI change imagery correlated to regions of F1 tornado damage, particularly in rural regions. Henebry and Ratcliffe (2003) used NDVI data from AVHRR to document the occurrence and persistence of hailstreaks in the Midwest from 1990 to 1999. Their findings indicated that some hailstreaks were visible in the NDVI composites up to 90 days after their initial occurrence. The National Aeronautics and Space Administration (NASA 2005) and the U.S. Geological Survey (USGS 2005) have used very high spatial resolution research instruments to qualitatively map a fairly large tornado damage track of the La Plata, Maryland, tornado southeast of Washington, D.C. (Strong and Zubrick 2004).

At times the destruction associated with extreme severe storms events is so extensive that it is visible in coarse-resolution imagery from instruments in geostationary orbits such as those on Geostationary Operational Environmental Satellites (GOES). A study by Klimowski et al. (1998) showed that a track of defoliation, approximately 120 km in length, caused by the 5–6 July 1996 Butte–Mead storm in western South Dakota was an obvious feature in the visible channel imagery from the *GOES-8* imager. Along the tracks of the storm, the destruction of range grasses resulted in higher albedo values compared to undisturbed surrounding areas and thus making it apparent in the *GOES-8* visible channel imagery.

Prior studies using satellite imagery to characterize or identify severe storm damage (Yuan et al. 2002; Bentley et al. 2002) mainly focused on high-resolution satellite data that were not readily available to the NWS damage assessment teams. These studies also used specialized image processing techniques to analyze satellite imagery, resources that are typically not available to WFO personnel for damage assessment. While such detailed analysis of high-resolution satellite imagery may be of considerable use for case study investigations, it is of limited practical use in postevent damage assessment. More recently, NASA (2005) and USGS (2005) have demonstrated tornado damage track detection capabilities with high-resolution earth resources sensors. The qualitative Web page presentations show the potential utility of such observing systems. This paper explores the use of near-real-time data from MODIS and Advanced Space-borne Thermal Emission and Reflection Radiometer (ASTER) instruments, some of which are made available to selected NWS Forecast Offices for evaluation and use in the operational environment as part of the NASA Short term Prediction and Research Transition (SPoRT) program (Goodman et al. 2004). This technology transfer initiative provides a risk reduction activity for operational use of future satellite sensor data streams.

This study uses NASA Earth Observing System (EOS) data to examine damage patterns associated with three tornadic events. In one case Landsat data are used as a surrogate for ASTER imagery. While the EOS satellite data do not provide the highest-resolution imagery available to the research community, they do provide detailed views of the earth's surface often not available to the NWS in real time. These satellite data are used to estimate tornado damage track length and width in order to demonstrate their contribution to damage surveys conducted by the NWS. The relationship between land cover type and the ability to detect tornado damage tracks in the satellite imagery is explored using land cover datasets, satellite imagery, and a satellite-derived vegetation index.

## 2. Background

### *a. The SPoRT center*

In 2002, NASA established the SPoRT Center at Marshall Space Flight Center in Huntsville, Alabama, as a vehicle to transition unique observing, modeling, and data assimilation capabilities (developed under the auspices of the NASA Science Mission Directorate, formerly the Earth Science Enterprise) to several NWS Forecast Offices (NWSFOs). This activity follows a "test bed" approach where 1) unique data are made available and 2) analysis techniques are developed and provided to NWS forecasters for real-time assessment and use. The SPoRT program also provides training on these new products and techniques and participates with the NWS forecasters and decision makers in the assessment of their capabilities. This interaction pro-

vides immediate feedback concerning the utility of the data in the operational environment. While this collaboration is facilitated by the collocation of the SPoRT Center and the Huntsville NWSFO, collaborations extend beyond the local office and include the Birmingham, Alabama; Nashville, Tennessee; Jackson, Mississippi; Mobile, Alabama; Miami, Florida; and Great Falls, Montana, forecast offices. This test bed approach has proven beneficial to the evaluation of the use of high-resolution satellite data from MODIS and other EOS sensors for a number of applications, including tornado damage assessment.

EOS observations from satellite instruments such as MODIS are collected in real time at a number of direct broadcast ground stations throughout the world. These stations receive line of sight data transmissions from several instruments on the *Terra* and *Aqua* satellites, providing local observations of surface and atmospheric features in real time. These ground stations run calibration and earth location software on the raw data files to produce level 1B data (calibrated radiances in the native satellite projection) equivalent to that archived at the various NASA Distributed Active Archive Centers (DAACs). The SPoRT program obtains MODIS data from two of these direct readout stations and provides the data to the NWS for analysis and use. ASTER data are currently not available in real time but can be obtained from the NASA DAAC for postevent analysis. The SPoRT program processes the imagery, subsets the data to meet the needs of individual NWS forecast offices, and stages the data and products on NWS regional servers (for the Southern Region this is in Fort Worth, Texas), where the satellite data are disseminated to the requesting NWSFOs. At the local offices, the data are ingested into the Advanced Weather Information Processing System (AWIPS), the NWS's decision support system (Friday 1994; Seguin 2002). MODIS data often are available to the forecast offices within 30 min of data collection.

### *b. Physical principles*

Satellite sensors measure reflected solar radiation in different spectral channels across the visible and infrared energy spectrum. The recombination of visible spectral channels into a picture or image creates a natural color scene similar to what is seen by the human eye. In this way the composite natural color satellite image can be used to detect variations in surface features associated with different land cover. In a similar way, the combination and use of additional channels in the near-infrared region of the energy spectrum (where reflected energy varies with the amount of photosynthetically active plant matter) allows for a spatial map of the vegetation or greenness over a region. This approach can provide a better delineation of surface feature variation particularly in the growing season.

The physical principle guiding the use of satellite data to detect tornado damage is based on the premise that the strong winds associated with a tornado or impact velocity of hail will change the physical characteristics of the surface in such a way as to alter the visible and infrared energy reflected from the surface as measured by the satellite sensor. These characteristics could be a change in the orientation of surface features or a physical change in surface reflective properties or both. The amount of surface damage produced by a tornado is certainly dependent on the strength of its winds, which may be somewhat correlated to its size, but the extent of surface damage is also dependent on the makeup of the underlying surface. A strong tornado will produce differing amounts of damage over open pasture, a dense forest, or a residential community. The damage produced by a tornado could be the complete destruction of a house in a residential area, the snapping of trees in a forest region, the uprooting of crops in an agriculture area, or minimal damage to grassland in a pasture or field. A damaged house will significantly change the pattern of reflected radiation measured by the satellite if observed with fine enough spatial resolution. Debris and soil scattered on vegetated surfaces by the storm can affect the reflectance as well. The damaged trees and uprooted crops will show a change in the amount of reflected radiation, and as the damaged trees and crops die and turn brown, they will exhibit a change in the vegetative properties or greenness of the surface as measured by the satellite. The pasture may not exhibit any changes in reflective properties that are detectable from space. The detection of storm damage tracks with satellite observations may be enhanced through the use of timely multispectral satellite imagery, which samples varying reflective properties of the surface at the appropriate spatial scales. Both qualitative (visual inspection) and quantitative analysis (application of mathematical techniques) of before and after images will provide supplemental data assessment information. However, additional variables such as land cover, storm intensity, time of year, and postevent sampling may influence the ability of the satellite data to detect storm damage signatures.

## 3. EOS data

### *a. MODIS data*

The MODIS instrument is carried on two NASA EOS satellite platforms, *Terra* and *Aqua*, which are in a sun-synchronous, near-polar, circular earth orbit at an

altitude of 705 km. The orbits of *Terra* and *Aqua* provide MODIS observation times at 1030/2230 and 1330/0130 (nominal local equator crossing time). MODIS acquires data in 36 spectral channels at nadir spatial resolutions from 250 to 1000 m for its visible and infrared channels, covering a swath width of 2330 km. Channels 1–7 are primarily used in remote sensing of land areas; in particular, vegetation imagery from MODIS channels 1 (0.620–0.670 $\mu$m), 2 (0.841–0.876 $\mu$m), and 6 (1.628–1.652 $\mu$m) were used individually and in an unsupervised classification scheme. Sixteen-day composites of 250-m NDVI values from MODIS (MOD13), routinely produced by the EOS science team and available from the EOS DAAC, were also used in this study. MODIS image data and products were remapped into a common coordinate system using the Man computer Interactive Data Access System (McIDAS; Lazzara et al. 1999).

### *b. ASTER data*

The ASTER is a high-resolution multispectral imager on board the NASA EOS *Terra* platform and collects data during the ascending node with equator crossing time of approximately 1030. Because of its narrow swath width (60 km) and orbital constraints, repeat coverage over a given region with ASTER imagery is nominally available every 16 days. However, ASTER data collection is not continuous, and the sensor acquires data only on demand. ASTER has 14 different spectral channels, which include three channels in the visible to near-infrared (VNIR), six in the shortwave infrared (SWIR), and five in the thermal infrared (TIR) regions at 15-, 30-, and 90-m resolution, respectively. The $\pm 24^\circ$ off-nadir pointing capabilities of the VNIR subsystem allow for the acquisition of imagery for targets of opportunity at up to 320 km away from the satellite subpoint. This study uses false color composites of the three VNIR channels to examine tornado damage on the ground. The false color composites were created by assigning colors at each pixel location with the red, green, and blue intensities in proportion to the radiance values of ASTER channels 2 (0.63–0.69 $\mu$m), 3 (0.76–0.86 $\mu$m), and 1 (0.52–0.60 $\mu$m) at that location. Atmospheric corrections were not applied to the ASTER data; however, the images were remapped into a common coordinate system using the McIDAS software.

### *c. Landsat ETM+ data*

The ETM+ sensor is carried on the *Landsat-7* satellite, which has an orbit similar to the NASA EOS *Terra* satellite, but with an earlier equator crossing time of 1000/2200. The ETM+ sensor is a multispectral imaging instrument with eight spectral channels: four channels in the VNIR, two in the SWIR, and one in the TIR region of the energy spectrum. The eighth channel is a 15-m panchromatic channel detecting energy in the wavelength range of 0.52–0.90 $\mu$m. The shorter-wavelength channels provide ground resolution of 30 m, while the infrared channels are available at 60 m. This study uses three-channel false color composite images created using channels 5 (1.55–1.75 $\mu$m), 4 (0.78–0.9 $\mu$m), and 3 (0.63–0.69 $\mu$m) to examine tornado damage. The false color composites were created by assigning colors at each pixel location with the red, green, and blue intensities in proportion to the radiance values of channels 5, 4, and 3 at that location. Atmospheric corrections were not applied but the Landsat data were remapped into a common coordinate system.

## 4. Observations of tornado tracks in satellite imagery

The various satellite imagery described above were used to examine damage associated with tornadoes and hail that occurred in Maryland and Missouri during 2002. These severe storm events occurred over geographical regions that vary in land cover. The 28 April 2002 event took place in the southwestern region of Maryland, an area with a mixture of urban (commercial/industrial and low-density residential), wooded land (mainly deciduous forest), and open fields used for pasture and row crops. The land cover in this region varies at fine scales, and no single land cover type dominates a given region. Although located in a rural community in Maryland, the region is not as isolated as the location of the 24 April 2002 event that occurred in the southeastern region of Missouri, a rural area that includes significant portions of the Mark Twain National Forest with relatively dense vegetation (deciduous and evergreen forest) undergoing rapid springtime greenup and growth at that time. The land cover in this region of Missouri varies at coarse scales. As will be discussed later, the spatial scale of land cover is significantly different over the Missouri region and this affects the ability to detect storm damage track signatures. Details of these events as determined from the NWS storm surveys and damage reports are presented in Table 1. The damage created by the tornadoes ranged from weak (F1) to severe (F4) on the Fujita scale and is representative of tornadoes with winds between 33 and 116 m s$^{-1}$. Damage tracks from these events ranged in length from 14.5 to 103.2 km and from 91 to 732 m in width. The goal of the following analysis is to demonstrate the role near-real-time satellite data

TABLE 1. Details of tornado tracks for the MD and MO events from the NCDC storm database.

| Date | Location | Max Fujita scale | Dimension | |
|---|---|---|---|---|
| | | | Length (km) | Max width (m) |
| 28 Apr 2002 | La Plata, MD | F4 | 103.2 | 594 |
| 24 Apr 2002 | Ellsinore and Marquand, MO | F4 | 66.2 | 594 |
| | | F2 | 14.5 | 732 |

may play in helping the NWS to conduct storm surveys. Map overlays of different resolutions were used on most of the following figures, allowing for appropriate levels of details, but occasionally resulting in differences in the location of roads and urban boundaries between the larger and the zoomed-in views. The map information was generated from the 2000 U.S. Census data and therefore any new construction between 2000 and the times of the satellite passes may have resulted in discrepancies between what can be seen in the satellite image and the map overlay.

### *a. Analysis of satellite imagery for the 28 April 2002 Maryland event*

In the early evening of 28 April 2002, a tornado formed about 30 km south of Washington, D.C., in Charles County, Maryland. This tornado stayed on the ground for over 50 min and traveled eastward covering 103.2 km. The tornado caused total property damage amounting to $115 million with 122 people injured and 5 killed. The tornado damage track and intensity map (AIR Worldwide Corporation 2002) are presented with the land cover image in Fig. 1. A complete description of the event is given by the National Climatic Data Center (NCDC 2005), the U.S. Department of Commerce (DOC 2002), and Strong and Zubrick (2004) and is summarized below. The supercell storm that produced the La Plata, Maryland, tornado moved across Virginia in the late afternoon and on into Maryland in the early evening where it also produced hail ranging in diameter from 1.5 to 4.5 in. at several locations north of the track of the tornado. The tornado was at its most intense stage as it passed through the town of La Plata, destroying most of the downtown businesses. Land cover varies between rural, residential, and industrial areas along the tornado track as indicated by the National Land Cover Data (NLCD) presented in Fig. 1 along with the tornado damage track as described by NCDC (2005) and DOC (2002). The NLCD dataset is a 21-category land cover classification derived from an unsupervised classification of Landsat data with a spatial resolution of 30 m (Homer et al. 2004; Vogelmann et al. 2001). The tornado track region is dominated by open fields (brown), regions of deciduous and evergreen trees (green), residential communities (yellow), and commercial and industrial areas (red). The land cover varies considerably (multiple class changes) over a few square kilometers throughout the tornado damage track region.

After formation near Rison, Maryland, the tornado moved eastward over open fields and scattered forested areas where it grew to F2 in strength (see Fig. 1a). It became an F3 tornado in a wooded area several kilometers west of La Plata and continued to gain strength as it passed through the residential and commercial areas of town producing F4 damage (see Fig. 1b). The width of the damage path in this region was estimated at nearly 600 m by the NWS survey team (DOC 2002). The tornado moved into the rural farm area of the county and it decreased in strength as it moved toward Benedict and then over the Patuxent River just south of the Route 231 bridge. It continued eastward, crossing Route 2/4, and toward the Chesapeake Bay where it weakened to a F1 tornado. Storm reports indicated additional storm damage on the east side of the bay (DOC 2002), possibly the result of the La Plata tornado.

Real-time high-resolution MODIS data are routinely available to several NWS forecast offices to help forecasters diagnose changing weather conditions. Figure 2 presents MODIS image data over a portion of southwest Maryland before and after the tornadic storm as it might have been viewed by NWS forecasters in AWIPS. Figure 2a shows the MODIS 250-m VNIR channel 2 imagery (base image and high-resolution insert for 24 April 2002, 4 days before the event). Channel 2 was used because it best highlighted the damage track. Also shown is a high-resolution MODIS 16-day NDVI composite product for the high-resolution insert region. The imagery over the same region for 1 May 2002 is displayed in a similar layout in Fig. 2b. By contrasting the before and after images from both the single-channel and NDVI products, there is evidence of the tornado damage track in the image as indicated by the linear feature running west to east through LaPlata in the high-resolution figure inserts of both channel 2 and the NDVI image. The feature is hard to discern, however, because of the variations in the surface reflec-

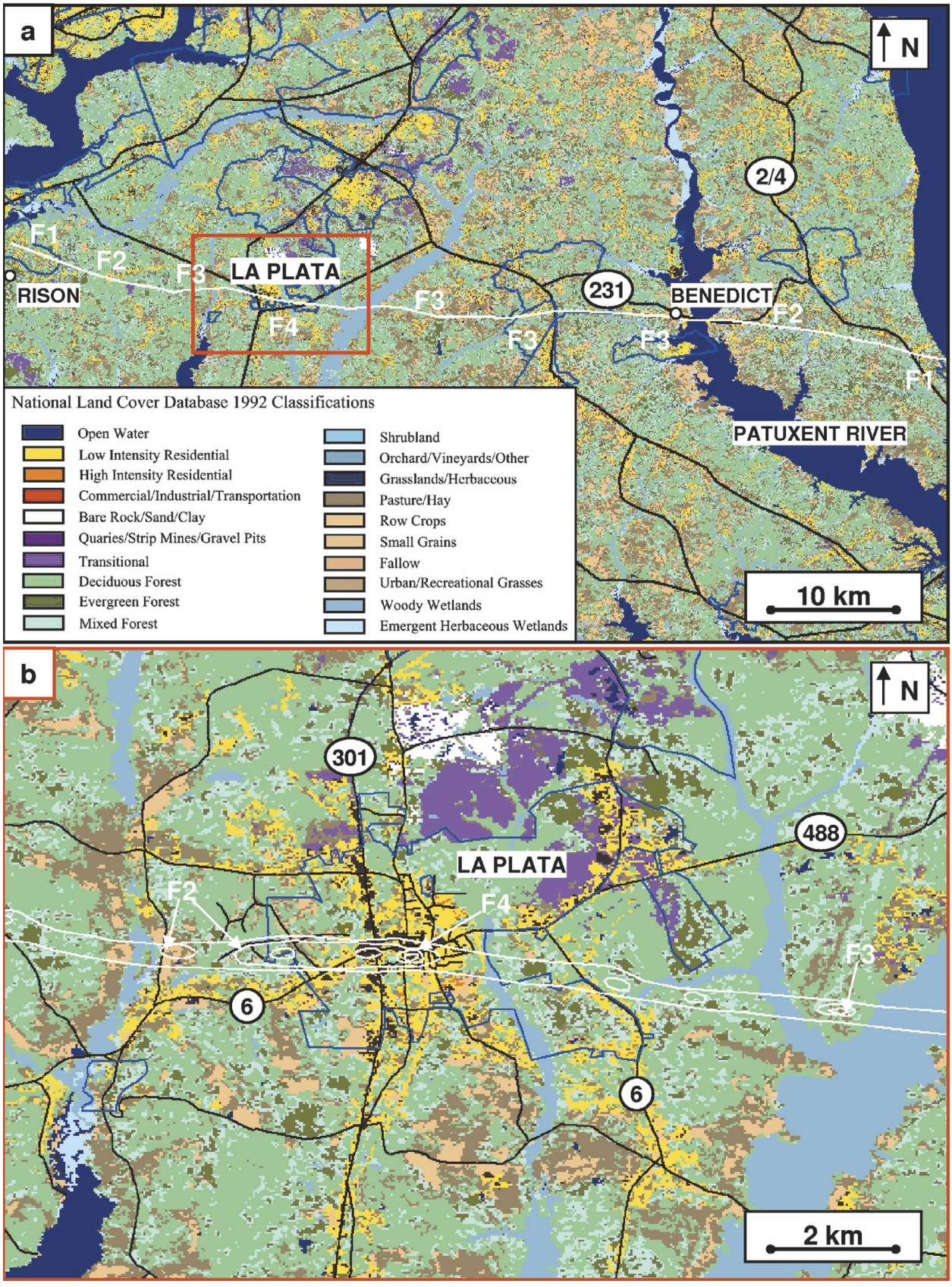


FIG. 1. NLCD images of (a) southwest MD and (b) La Plata as outlined by the red box in (a). The location of the tornado track is shown in white in (a), (b), and the intensity (F1–F4) is indicated in (b) by the concentric ovals.

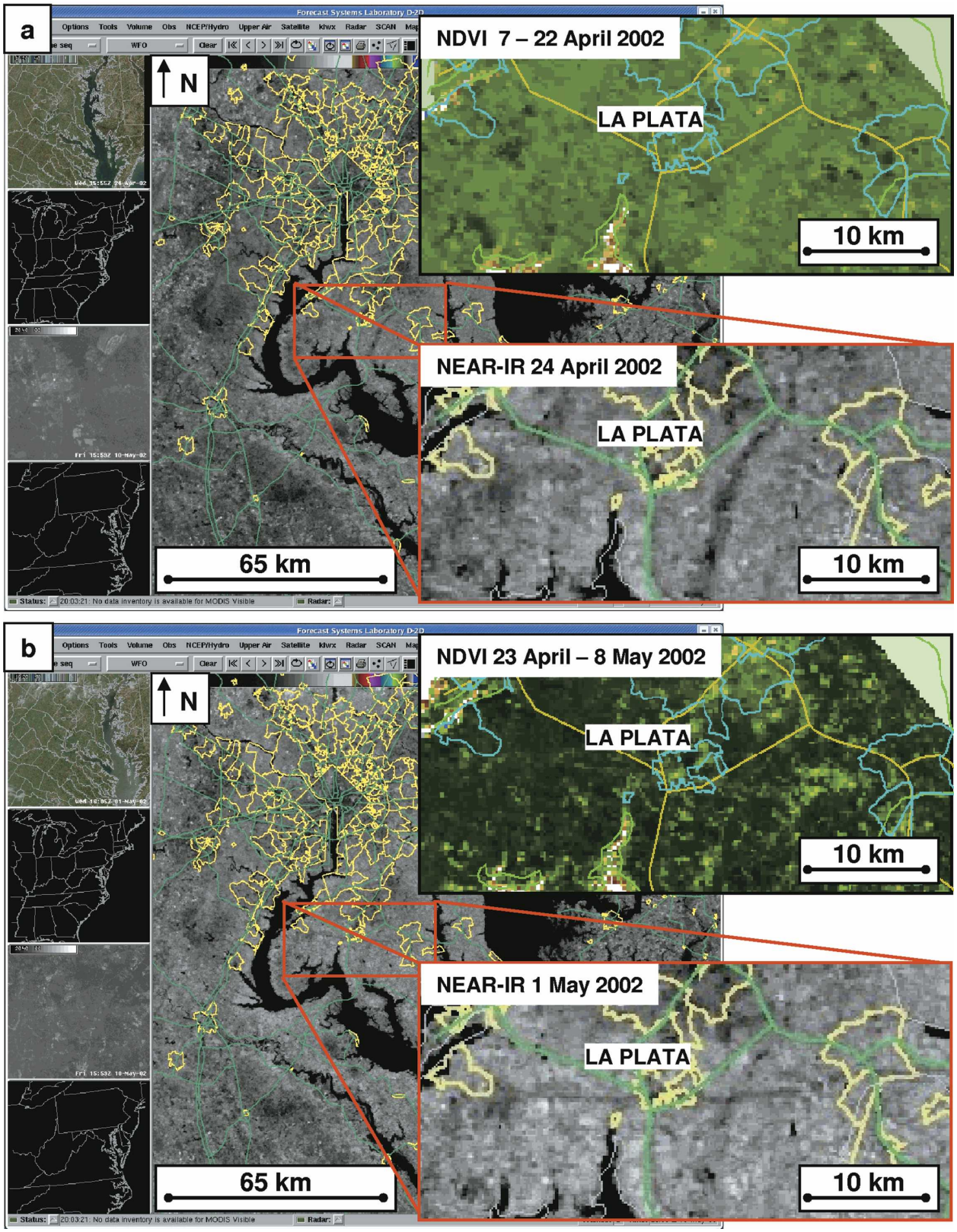


FIG. 2. MODIS near-infrared (channel 2) imagery of southwest MD as seen in the NWS display system AWIPS, with a high-resolution inset centered on La Plata, and an accompanying NDVI image of the same inset region. Images from (a) before and (b) after the 28 Apr 2002 tornadic storm.

TABLE 2. Mean and std dev of MODIS-derived 16-day composite NDVI observed within the tornado and hail damage tracks and the immediate surroundings.

| Location | Feature | Time period | 16-day composite NDVI | |
|---|---|---|---|---|
| | | | Mean | Std dev |
| La Plata, MD | Tornado track | 8–23 Apr 2002 | 0.74 | 0.06 |
| | | 24 Apr–9 May 2002 | 0.75 | 0.11 |
| | Background | 8–23 Apr 2002 | 0.80 | 0.07 |
| | | 24 Apr–9 May 2002 | 0.86 | 0.07 |
| Ellsinore and Marquand, MO | Tornado track | 8–23 Apr 2002 | 0.61 | 0.05 |
| | | 24 Apr–9 May 2002 | 0.67 | 0.08 |
| | Background | 8–23 Apr 2002 | 0.73 | 0.05 |
| | | 24 Apr–9 May 2002 | 0.84 | 0.04 |
| | Tornado track | 8–23 Apr 2002 | 0.71 | 0.04 |
| | | 24 Apr–9 May 2002 | 0.80 | 0.06 |
| | Background, track | 8–23 Apr 2002 | 0.79 | 0.03 |
| | | 24 Apr–9 May 2002 | 0.84 | 0.04 |
| | Hail swath | 8–23 Apr 2002 | 0.57 | 0.08 |
| | | 24 Apr–9 May 2002 | 0.67 | 0.10 |
| | Background, hail swath | 8–23 Apr 2002 | 0.81 | 0.03 |
| | | 24 Apr–9 May 2002 | 0.85 | 0.05 |

tance and vegetation properties due to the varied land cover as indicated by the NLCD images in Fig. 1.

To quantify the reflective signature difference between the tornado track and the surrounding undamaged region, Table 2 presents the mean and standard deviation of the MODIS-derived 16-day composite NDVI for selected portions of the image. The tornado track values come from the NDVI images (inserts in Figs. 2a and 2b) based on the damage track shown in Fig. 1. The values for the surrounding areas are computed using samples obtained from a strip of area bordering the track and extending to 3 km on either side of the tracks. The NDVI comparison between the two regions indicates that the nondamage region NDVI values are consistently higher than for the damage track region. This shows that destruction of vegetation by severe storms contributes significantly to the storm damage track signal observed in satellite imagery. Note that the NDVI difference between the track and the surroundings is observable even a few weeks after the event. This feature is consistent with the findings of Parker et al. (2005) and others.

Yuan et al. (2002) showed that changes in satellite-derived NDVI imagery between two times can highlight tornado damage regions quite well. The composite NDVI imagery (in Fig. 2) offers the advantage of a cloud-free view of the track compared to single-channel imagery that may contain clouds. Figure 3a presents an image of the differences between the NDVI composite imagery displayed in Fig. 2 for the La Plata region. The tornado track is evident but not obvious in the NDVI difference image. The variation in land cover and corresponding vegetation changes during the spring greenup period, combined with the compositing process, may explain the difficulty in detecting the tornado track in the difference imagery. Applying the difference imaging approach to the MODIS 250 m channel 2 imagery displayed in Fig. 2 produces a significantly better depiction of the tornado track as indicated in Fig. 3b. The difference image shows a linear feature in nearly the exact location of the track in Fig. 1a. There is also a broader linear feature in the difference image in a mixed forested and residential region about 7 km north of La Plata that may be evidence of a second tornado or a region of hail damage as indicated in the storm reports. Other alternative products such as the rotational track product derived from Doppler radar azimuthal shear data (Stumpf et al. 2003) used in combination with the satellite data could better isolate additional regions for storm damage assessment. The single VNIR channel difference image better detects the tornado damage track (over the NDVI difference image) because of its exclusive use of the 250-m data in a single spectrally narrow channel at two specific times, and more directly measures changes in vegetation. The combination of the three 250- and 500-m channels and the broader spectral coverage in the NDVI image blurs the spatial information content in the difference image.

To further explore the quantitative detection of damage paths associated with the La Plata storm, an unsupervised classification scheme of Levine and Shaheen (1978) was applied to the MODIS channel 2 and channel 6 (reflective infrared) imagery. The algorithm identifies statistically distinct clusters of pixels in the multispectral imagery and assigns the pixel membership to groups or regions. Membership is determined by calcu-

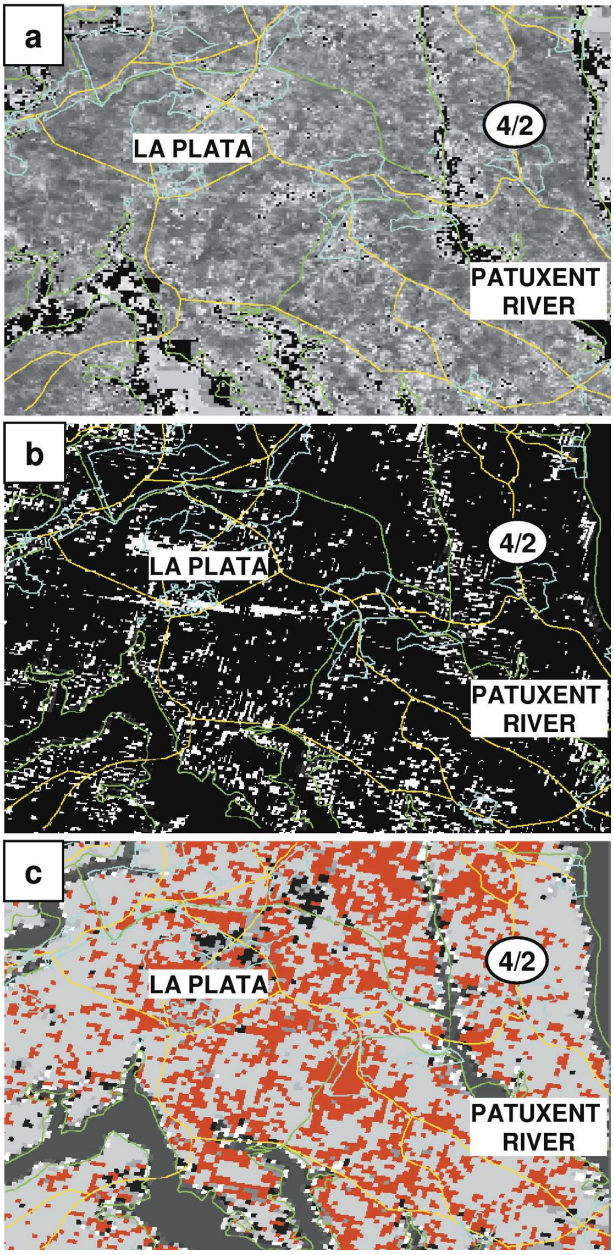


FIG. 3. Imagery of southwest MD of (a) the difference between 16-day MODIS NDVI imagery from 7 to 22 Apr and 23 Apr to 8 May 2002, (b) the difference between 24 Apr and 1 May 2002 from MODIS channel 2, and (c) unsupervised classification of 1 May 2002 from MODIS channels 2 and 6.

lating how the addition of a pixel to a particular group alters its mean and standard deviation. These channels were chosen because vegetation is highly reflective in channel 2 compared with bare soil, while in channel 6 bare soil is more reflective compared to vegetation. The unsupervised classification image is presented in Fig. 3c. One of the identified classes (shown in red) includes the majority of the pixels located within the tornado track and suspected hail and second tornado damage regions. Note that even though the classifier identifies a majority of the pixels in the tornado damage track as a separate class, it also groups a number of other pixels in the imagery as belonging to the same class. Thus, the damage track does not stand out as a unique feature in the classification image. The unsupervised classifier was used to identify pixels belonging to the damage tracks and to contrast them against the surroundings, not to identify the different classes of land use found within the scene. Thus, an accuracy analysis of the unsupervised classifier was not performed. Despite its relatively poor performance here (does not exclusively isolate only the storm damage tracks), the detection accuracy (ability to identify and cluster features with similar spectral characteristics) with this approach has exceeded 90% as a prior-use classifier to detect clouds (Nair et al. 1999).

In addition to identifying the location of tornado damage tracks, the NWS storm damage survey teams estimate the length and width of the affected (damage) areas and an estimate of the intensity of the winds based on the damage rated on the Fujita scale. While the tornado damage in this region is best seen in MODIS channel 2, the damage track is only apparent in the MODIS data for a portion of the 103-km length reported by the NWS storm reports. To estimate this length, the MODIS imagery was registered and each pixel was remapped to 250-m resolution projection. McIDAS distance routines were then used to calculate the straight-line distance between the beginning and ending points of the damage track (determined subjectively by viewing the imagery) in the MODIS imagery. The length of the Maryland tornado track estimated from the MODIS satellite imagery is about 33 km, as indicated in Table 3. While this is significantly shorter than the reported pathlength for the entire storm, it is only about 6 km shorter than estimated by the NWS damage survey team for Charles County (NCDC 2005) where the tornado was at its strongest. The maximum discernable damage path width in the satellite imagery is no more than two MODIS pixels (about 500 m), consistent with the damage survey report of 594 m. It appears that the damage caused by the tornado during the early and later stages of the tornadic storm is not extensive enough to be visible in the 250-m MODIS data, the difference imagery, or the classified imagery. This is consistent with the F0–F1 intensities reported for the tornado track in Calvert and Dorchester Counties (DOC 2002; NCDC 2005). The failure to detect these damage regions is likely the result of less damage

TABLE 3. Satellite estimates of the pathlength and width for the tornado tracks of the MD and MO events.

| Date | Location | Sensor | Dimension | |
|---|---|---|---|---|
| | | | Length (km) | Max width (m) |
| 28 Apr 2002 | La Plata, MD | MODIS | 33 | 500 |
| | | ASTER | 33 | 1275 |
| 24 Apr 2002 | Ellsinore and Marquand, MO | MODIS | 58 | 750 |
| | | Landsat | >45 | 600 |
| | | MODIS | 22 | 750 |
| | | Landsat | 21.5 | 690 |

caused by the weaker tornado and the high variability in land cover over the region.

ASTER data from 10 May 2002 were obtained over the La Plata, Maryland, tornado region and are presented in Fig. 4 as a three-channel false color composite image. Figure 4a shows the imagery at 60-m resolution. Although the ASTER instrument has off-nadir view capabilities, the La Plata track viewing angle was on average only 2°–3° off nadir. The details seen in the ASTER imagery are astonishing. Compared with MODIS imagery, the tornado track from the Maryland event shows up as a very striking feature (deep purple region) in the ASTER images. Undisturbed vegetated regions appear green. A distinct damage path is seen beginning on the left of the ASTER image running through La Plata and continuing in an east-southeast direction. There is no apparent track on the east shore of the Patuxent River. The ASTER imagery was remapped to 15-m resolution using McIDAS and track length estimates were calculated with the appropriate distance routines. Track width was determined by summing the 15-m pixels. The total length of the tornado track observed in the ASTER satellite imagery is approximately 33 km, which is consistent with the MODIS observations (Table 3). However, the ASTER imagery does not provide coverage to Rison where the tornado initially formed. The width of the damage track ranges from 90 to 1275 m in the ASTER imagery. This estimate is wider than that reported by the storm reports. Estimating the track width from satellite data is more difficult in urban regions (where the land cover varies significantly), since variations in land cover can be confused for storm damage and may have contributed to the larger satellite estimates. The variation of land cover in urban regions can also contribute to the false detection of damage tracks without the use of other corroborating information.

Additional details on the variation in length and width of the damage track can be seen in the 15-m full-resolution portion of the false color composite ASTER scene centered on La Plata and shown in Fig. 4b. Roads, subdivisions, and regions of varying land cover are quite obvious in the 15-m imagery as are details of the damage track. On the left side of the image, the damage track is about 570 m wide (38 pixels) and shows a slight change in direction as it approaches Morgans Ridge Road to the west of town. This is consistent with the damage track presented in Fig. 1b that shows a similar turn in the track. The width of the damage track increases to 795 m (53 pixels) at the La Plata downtown area and remains about 800 m wide past Route 6 and into the forested region to the east of town. This is consistent with the F2 and F3 damage locations in Fig. 1b. There are several regions of more severe tornado damage between Route 6 and the wetland area on the right side of the ASTER image. Image estimates of track damage on the right side of the image are 1275 m (85 pixels) and correspond to the woody wetland area with F3 damage in Fig. 1b. While the variation in track width detected by ASTER is a reflection of the changing intensity of the tornadic storm or of the changing damage signature for different underlying land cover types is unknown, the most striking signatures in the ASTER data appear in forested regions to the west and east of town and not in the town itself. Also note that the damage track in the urban area provides less contrast against the natural background because the reflectivity signatures along the damage track are similar to those of urban areas and bare ground, possibly limiting the detection of tornado damage tracks using our techniques in urban areas. High-resolution imagery from the *Earth Observing-1* (*EO-1*) Advanced Land Imagery (Bryant et al. 2003) supports this analysis (StormCenter Communications 2005), implying that the underlying land cover may be a key factor in the detection of tornado damage in satellite imagery.

Qualitative verification of this damage area is seen by comparison of the ASTER image with an oblique aerial photo in Fig. 5 taken on 30 April (2 days after the storm). The aerial photo shows the variation in the width and the change in orientation of the tornado damage track just before Morgans Ridge Road, consistent with the high-resolution ASTER data and the damage track in Fig. 1b. The photo also shows damage

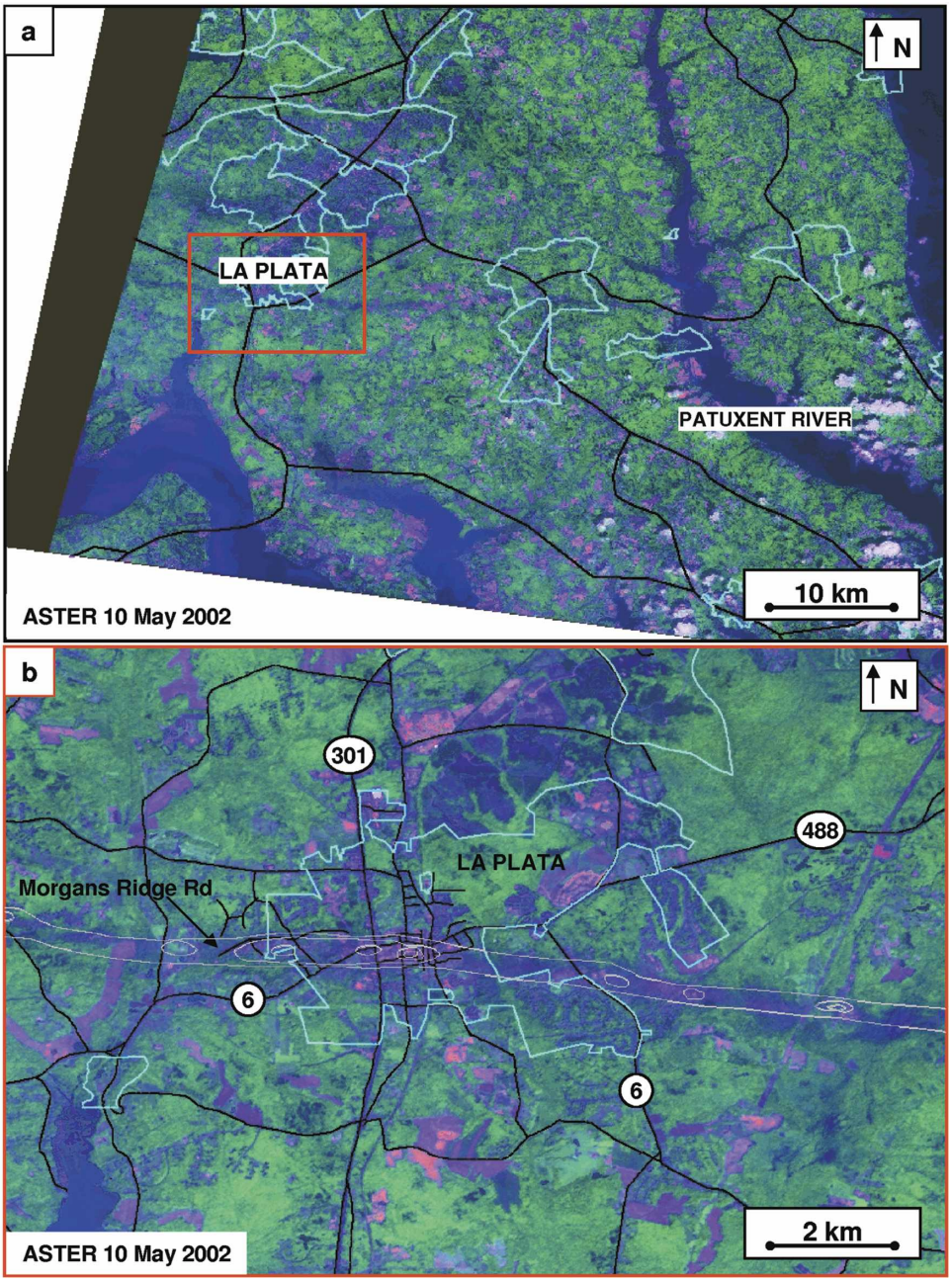


FIG. 4. ASTER three-channel false color composite image of southwest MD on 10 May 2002, showing the tornado damage tracks at (a) low resolution for the same region as shown in Fig. 1a and (b) 15-m resolution for the region centered over La Plata as outlined by the red box in (a) and as shown in Fig. 1b.

to La Plata and to the forested region to the east of the town.

### *b. Analysis of satellite imagery for the 24 April 2002 Missouri event*

On 24 April 2002, a strong cold front moved through the central plains and triggered widespread severe thunderstorms across Missouri and Illinois. Several of these thunderstorms produced tornadoes across southeast Missouri, which is the focus of the analysis and discussion below. The Ellsinore tornado touched down just west of Van Buren damaging two business establishments with F2 winds. Figure 6a shows the reported tornado damage track (NWS 2005) and land cover map

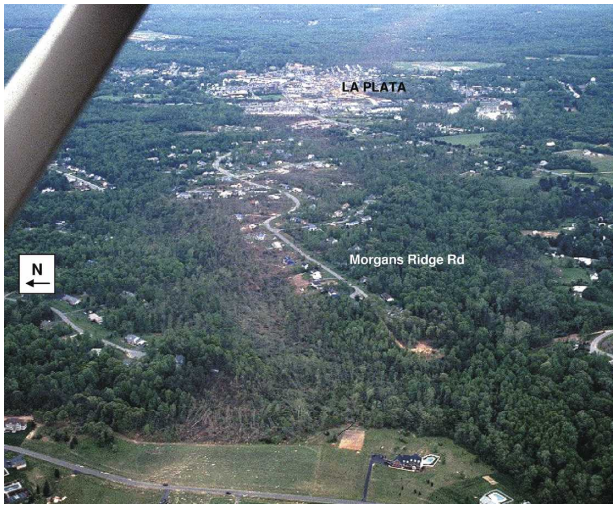


FIG. 5. Aerial photograph taken on 30 Apr 2002 of the tornado damage path looking east toward La Plata. (Courtesy of T. Marshall.)

for the region. The tornado moved southeast though hilly, forested terrain encountering the community of Ellsinore, where its F4 intensity winds destroyed seven businesses. The tornado moved into the Mark Twain National Forest and passed north of Poplar Bluff where it dissipated over farmland about 10 km northeast of the city. The NWS storm survey listed F4 storm damage in several locations with a total of 63 houses destroyed, 58 others were seriously damaged, and significant timber losses occurred in the national forest for a total loss estimate of over $45 million. The total damage track length was 66.2 km. The damage track varied in width from about 297 m for the region around Ellsinore to about 594 m in parts of the national forest (Table 1).

The second tornado of interest (the northernmost track in Fig. 6a) formed just west of Highway 67. The tornado moved in an easterly direction through a densely wooded area and through the town of Marquand where 6 houses were destroyed and 32 houses were damaged. The pathlength of the tornado was estimated at 14.5 km by the survey team with a width of around 732 m. Damage assessment was not conducted to the west of Highway 67 or to the east of Marquand, probably because of limited resources by the local WFO. Alternative sources of data, such as EOS imagery and rotational tracks derived from Doppler radar (Stumpf et al. 2003), could have provided additional information for the assessment of storm damage. An associated hail storm produced a damage path over 65 km long and 5 km wide to the west and south of the tornado track (Missouri Department of Conservation 2005).

Figure 7a presents the MODIS 250-m visible imagery (channel 1) over this region of Missouri for 23 April 2002 (Fig. 7a, 1 day before the storm) and 14 May 2002 (Fig. 7b, nearly 3 weeks after the tornado) as it would be viewed by the NWS in AWIPS. Of all the MODIS surface sensing channels, the 250-m channel 1 imagery best detected the tornado tracks for the Missouri region. The image inserts (offset from the base image) show high-resolution MODIS visible imagery centered on each tornado track region. Linear features associated with both tornado tracks are obvious in the 14 May imagery. In comparison to Fig. 6a, these features coincide with the tracks determined by the NWS storm survey with a few exceptions. For the Ellsinore tornado, the tornado track is not evident in the MODIS imagery over the agricultural region to the northeast of Poplar Bluff. For the Marquand tornado, the MODIS data identify tornado damage in the forested regions that extend beyond the path documented in the storm reports in each direction (see Figs. 6a and 7b). Additionally, a large damage area in the forested region to the west and south of the tornado track corresponding to a hail damage region [the white outline in Fig. 6a; Missouri Department of Conservation (2005)] is evident in the MODIS imagery. The NDVI composite image values for the storm damage regions were contrasted with the nondamaged areas and are presented in Table 2. The storm track regions are again characterized by lower NDVI values. The overall values are lower for the hail regions in Madison County but show the same relative trend.

Figure 8a presents an NDVI composite difference image to help quantify the detection of the tornado tracks in the MODIS imagery. Procedures identical to those of the Maryland case were applied to the data. The NDVI difference image nicely identifies the tornado damage tracks for both the Ellsinore and Marquand tornadoes. Other features such as rivers and streams also show up in the difference image since heavy rains between the observation periods significantly affected the scene reflectance values, and therefore the NDVI values, for these regions. New road construction for the Highway 60 bypass to the west of Ellsinore also shows up in these difference images and in the Landsat data in Fig. 9. The erroneous detection of these features in both manual and automated damage track detection schemes will contribute to the false detection of damage tracks and lower the overall detection accuracy with MODIS data. The hail damage area is well identified in the NDVI difference image. The detection of hail damage in the NDVI difference imagery is consistent with the findings of Henebry and Ratcliffe (2003) and Bentley et al. (2002). Parker et al. (2005) also indicates the detection of hail damage with a time

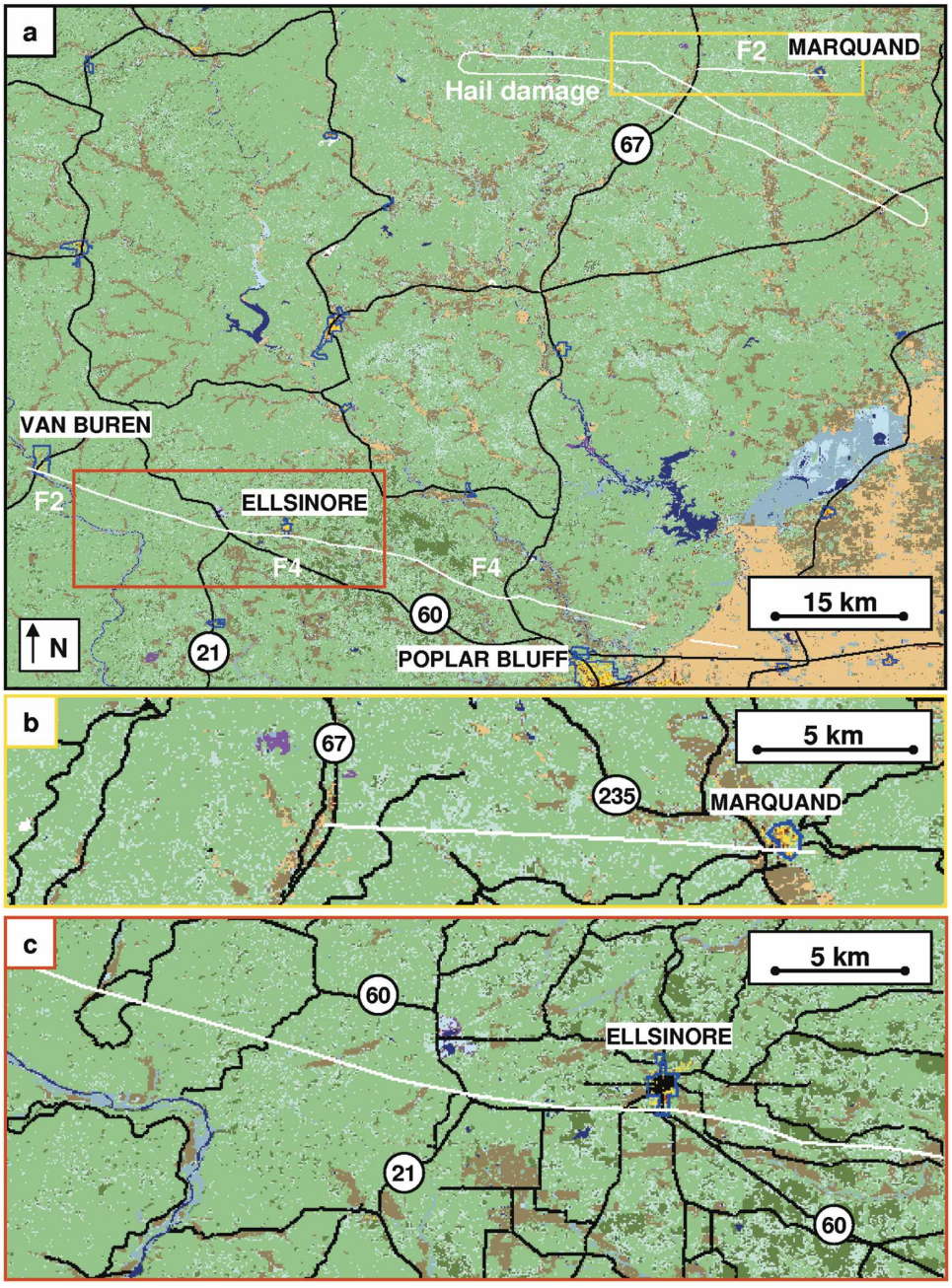


FIG. 6. NLCD images of (a) southeast MO with hail damage region indicated by the closed outline in white and of (b) Marquand and (c) Ellsinore as outlined by the yellow and red boxes, respectively, in (a). The locations of the tornado tracks are shown in white.

sequence of MODIS imagery. The unsupervised classification scheme was applied to MODIS channels 2 and 6 (which contrast vegetated and nonvegetated surfaces) and is presented in Fig. 8b for the southeastern Missouri region covered by Fig. 6a. Unlike the La Plata tornado, the scheme nicely identifies most of the tornado and hail damage regions without significant overclassification of other features. For the Ellsinore tornado, the damage region is highlighted from near Van Buren across Highway 67 and to the north of Poplar Bluff (see map and track in Fig. 6a). For the Marquand tornado, the track is identified between Highway 67 and Marquand and the previously unidentified region to the west. Portions of the hail damage region are also

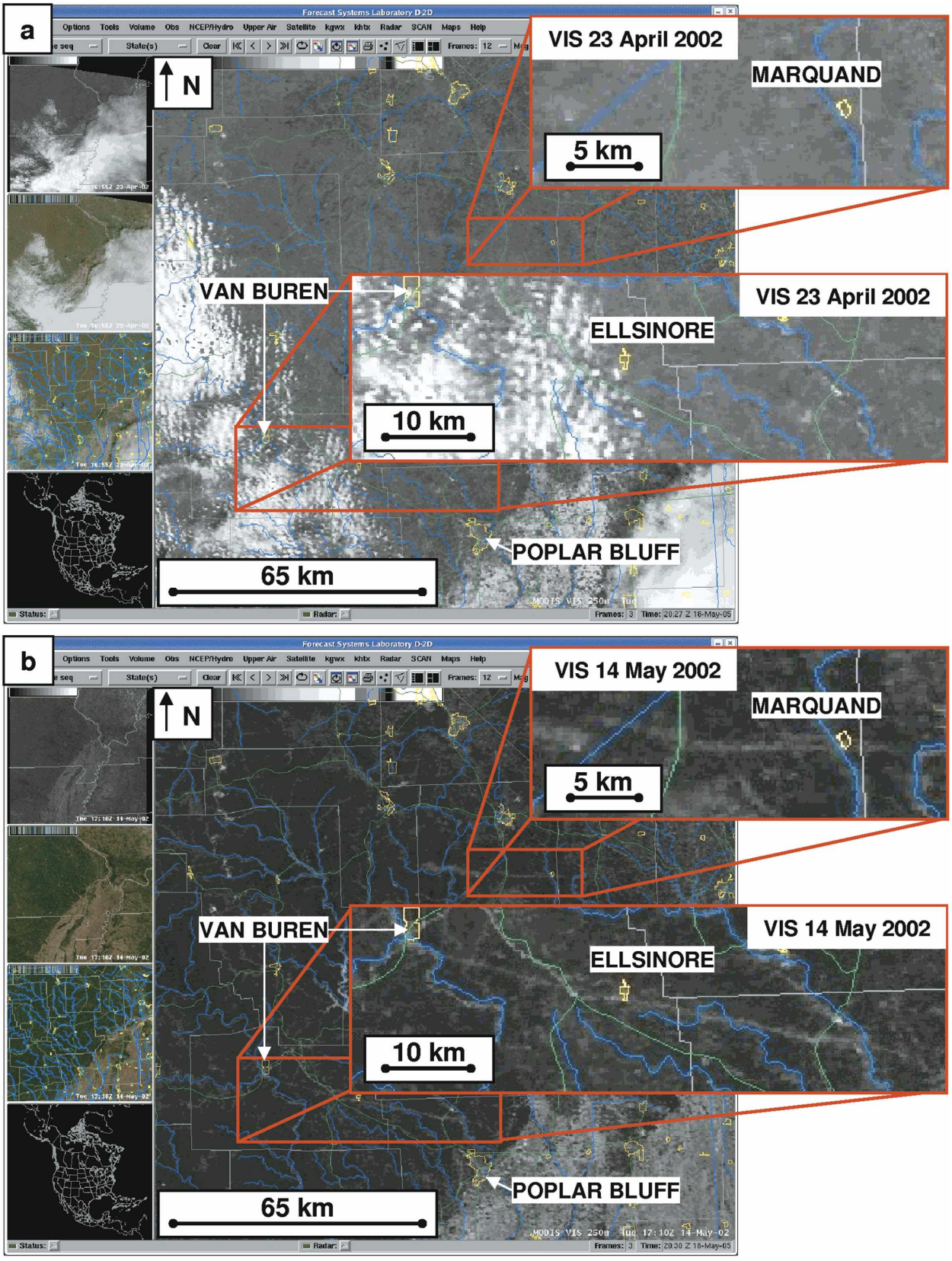


FIG. 7. MODIS visible (channel 1) imagery of southeast MO as seen with the NWS display system AWIPS, with high-resolution inserts centered on Marquand and Ellsinore. Images from (a) before and (b) after the 24 Apr 2002 tornadic storm.

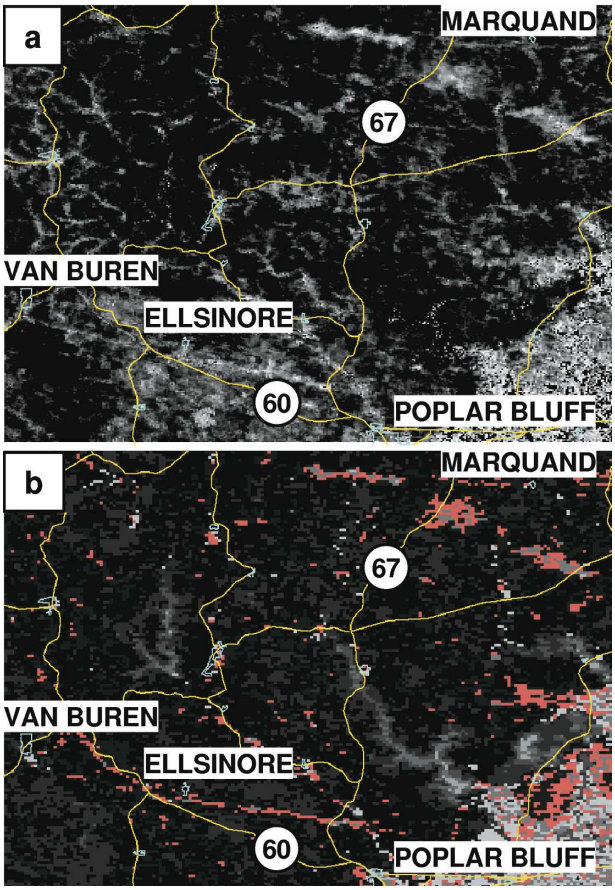


FIG. 8. Imagery of southeast MO for (a) the difference between 16-day MODIS NDVI imagery from 7 to 22 Apr and 23 Apr to 8 May 2002 and (b) unsupervised classification of 14 May 2002 from MODIS channels 2 and 6.

assigned to this class as the disturbed vegetation for the storms leaves an identifiable signature in the two MODIS channels. These damage tracks may be more readily detected using MODIS data than those of the La Plata tornado because of the underlying land cover. The Missouri tornados occurred in a region dominated by hardwood and evergreen forests, with just small breaks in this land cover around rivers and streams. For this region of Missouri, the land cover varies over a much coarser scale (a few class changes), over several hundred square kilometers, than for the Maryland region.

Tornadoes and hail storms may often go undetected and the extent of their damage is often not well documented. Access to large regions of the rural Missouri countryside (as well as other regions) is limited by the few roads in the region. Operational workloads of WFO staff limit the amount of time they can spend on damage assessments. Storms may cross over from one office's warning area to another, but the coordination of damage assessment from such storms may not occur between offices. Alternative data sources such as the satellite or derived radar products can provide preliminary damage track information and guidance to the WFO on where to concentrate their damage assessment efforts as discussed by Speheger et al. (2002).

To estimate tornado track length, the MODIS channel 1 image was registered and each pixel was remapped to 250-m resolution using McIDAS. McIDAS distance routines were used to calculate the straight-line distance between the beginning and ending points of the damage track in the MODIS imagery. The Ellsinore tornado track is apparent in the MODIS imagery for 58 km (Table 3). This estimate coincides fairly well with the location and tornado pathlength reported in the NWS damage survey (66.2 km) as presented in Table 1. The biggest discrepancy occurs near the end of the track on the north side of Poplar Bluff when the tornado was most likely in a dissipating stage. The spatial change in land cover over the region to the northeast of the city may have added to the difficulty of detecting the damage track. The width of the damage track estimated from the MODIS data varied from 250 to 750 m (one to three pixels). Based on the MODIS satellite imagery, the initial section of the tornado damage track between Van Buren and Ellsinore was not as wide as the remainder of the damage region, which is consistent with ground observations of tornado damage in these regions. However, note that accurate determination of tornado track width from MODIS satellite imagery is limited by the 250-m sensor spatial resolution.

The MODIS-derived estimate of damage track length for the Marquand tornado is 22 km compared to the ground observation of 14.5 km. It appears that a 5.5-km segment at the beginning and a 2.0-km segment at the end of the damage track may not have been identified by the damage survey team. The MODIS damage track width reaches 750 m (three pixels) to the west of Highway 67.

The ASTER instrument on the *Terra* satellite did not collect data over the tornado damage regions of southeast Missouri at any time close to the storm event. In fact, since ASTER data collection must be scheduled in advance, regular data collection for any given region is uncommon and in many cases repeat coverage of a given region does not exist. However, the Landsat ETM instrument did make an overpass of the Missouri tornado damage region on 9 May 2002. The three-channel false color composite Landsat image is shown in Fig. 9 for the coverage regions in Figs. 6a–c. The resolution of each pixel in this swath of Landsat data is 30 m. The tornado tracks are nicely delineated in both

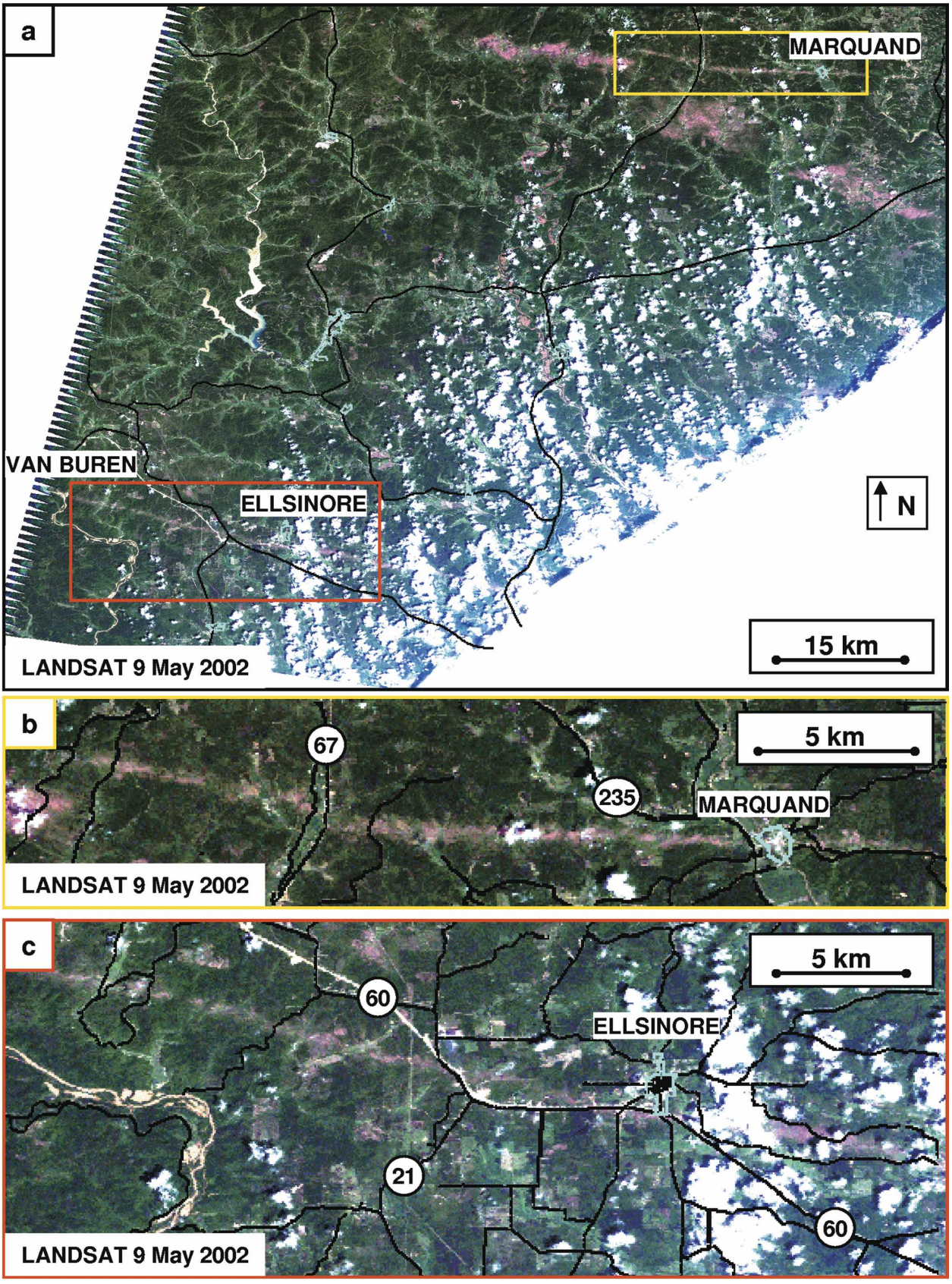


FIG. 9. LANDSAT three-channel false color composite image over southeast MO on 9 May 2002, showing the tornado damage tracks at (a) low resolution for the same region as shown in Fig. 6a and 30-m resolution over (b) Marquand and (c) Ellsinore as shown in Figs. 6b and 6c and outlined by the yellow and red boxes in (a), respectively.

the low-resolution image displayed in Fig. 9a and in the detail imagery in Figs. 9b and 9c. For the Ellsinore storm, the Landsat data confirm the MODIS tornado track identification from Van Buren and past Ellsinore to the edge of the scene (Figs. 9a and 9c). From this Landsat image the tornado track length was determined to be at least 45 km, but portions of the track continue off the image or are obscured by clouds. The Ellsinore tornado path width varies from approximately 180 m to the west of Ellsinore to about 600 m to the east. The estimated widths from the Landsat data are fairly consistent with the widths from the damage survey maximum width findings listed in Table 1.

The false color three-channel color composite from Landsat over the Marquand tornado region is presented in Figs. 9a and 9b and confirms the existence of tornado damage regions beyond those reported in the storm surveys. The entire damage path observed in the Landsat data is estimated to be about 22 km. The width of the damage regions varies between 210 and 690 m (Table 3), the widest section just west of Highway 67. This is consistent with the MODIS observations. The damage track is not clearly evident to the west of Marquand, either as a result of more agricultural land cover in the Caster River valley (note bright green color in the image) or of a weakening of the tornado. The damage track is more apparent to the east of the town for several kilometers. The Landsat data also identify three large regions of possible hail damage to the west and south of the tornado track (see Figs. 6a, 9a, and 9b). These image features are not contiguous as indicated in the damage reports (Fig. 6a; Missouri Department of Conservation 2005). The Landsat image shows distinct regions of hail damage and path widths that exceed 6 km for the region south and east of Highway 67. The unusual position of this hailstreak to the right of the tornado track may indicate that the tornado and hail damage occurred from two different storms. The use of other data sources and products such as the radar-derived rotational track map could help to identify this.

## 5. Discussion

This study explored the possibility of using near-real-time medium- and high-resolution satellite imagery from the NASA EOS satellites to survey tornado and hail damage tracks on the ground. It was found that, depending on the nature of land cover and severity of the damage, tornado damage tracks may be evident in both ASTER (and Landsat) and MODIS satellite imagery. In areas of dense vegetation (standing trees in particular) the scar patterns caused by tornadoes and hail show up very clearly in the satellite imagery, while in areas of open grassland, the scar patterns are not as obvious in the medium- and sometimes even high-resolution satellite imagery. Finescale variations in land cover between vegetation classes or between vegetation and urban or industrial use confuse both manual (visual) and automated detection of damage tracks. Comparison of 250-m visible and NIR imagery derived from MODIS data, before and after a tornado event, may be sufficient to detect damage tracks from F2 and stronger tornadoes during the growing season in forested regions. Tornado damage tracks are also identifiable in 16-day NDVI composite imagery derived from 250-m MODIS imagery. The NDVI imagery may bring out additional features not apparent in a single image, and has the advantage of providing a cloud-free view of the tornado track region, although it is not available in real time.

The use of more automated detection approaches such as difference imagery and image classification schemes was marginally successful at identifying the damage tracks from the more intense tornadoes and hail storms. Although NDVI difference imagery identified vegetation changes in the damage path regions, these signatures were often masked by or confused with natural vegetation changes during the observation period. An unsupervised classification approach identified only portions of the damage track regions subjectively discernable in the imagery, and also included some undisturbed features in the same classification as the storm damage.

Damage tracks can be very prominent features in high-resolution satellite imagery such as from ASTER and Landsat. This study showed that medium- and high-resolution EOS satellite imagery could potentially be a valuable tool during damage surveys conducted by the NWS in the aftermath of a severe storm, by providing additional insight into the location, length, and width of the tornado and hail damage areas. The detection of previously unidentified segments of a damage tracks caused by the 24 April 2002 Marquand, Missouri, tornado with MODIS data demonstrates the utility of satellite imagery and other readily available data sources during damage surveys. The high-resolution satellite imagery provided a better delineation of the size and coverage of a nearby hail damage region. However, even for the some very high resolution imagery, the ability to detect tornado tracks in satellite imagery appears to be dependent on the nature of the underlying surface and on the severity of the tornadic storm. The likelihood of the EOS satellite imagery detecting storm damage regions increases with the size and severity of the storm. Damage from large storms in regions of uniform land cover and growing vegetation

(such as forests) has the greatest probability of being detected with MODIS data. Use of other nontraditional products can reduce the false detection rate that can occur with the more automated approaches with satellite data. A more extensive study is required to quantify detection accuracy using the EOS data.

The real-time NASA EOS satellite observations are just one of a number of new resources being evaluated to assist NWS forecasters and survey teams in assessing the affects of severe storms. Scientists at the National Severe Storms Laboratory are developing a variety of new radar techniques to investigate severe storms, including a rotational track product that has also been used to verify the location of tornado damage tracks (Stumpf et al. 2003). Tornado and hail damage surveys consume valuable resources of the individual WFOs. Limited staff and many other responsibilities restrict the staff and time available to conduct these surveys (Speheger et al. 2002). Routine EOS satellite data and advanced radar techniques available to the WFO via AWIPS can focus the damage surveys and maximize resources. Additionally, satellite observations can provide coverage beyond a single WFO warning area, allowing for the collection of tornado and hail damage information outside the local office warning area.

MODIS satellite imagery from the NASA EOS *Terra* and *Aqua* platforms is available operationally in near–real time to a limited number of NWS Forecast Offices for use in short-term weather forecasting and for post-storm damage surveys. ASTER data can be provided to these offices, if available, but not in real time. The Visible Infrared Imager Radiometer Suite (VIIRS; Schueler 2003) to be launched on the National Polar-orbiting Operational Environmental Satellite System (NPOESS; Nelson and Cunningham 2002) beginning with the NPOESS Preparatory Project satellite in 2007 will continue many of the observing capabilities now performed with MODIS. The VIIRS will have numerous VNIR channels providing 375-m resolution imagery operationally to the NWS forecast centers. The use of MODIS data in the SPoRT program (Goodman et al. 2004) serves as a risk reduction activity for the future operational use of VIIRS data and that of the Advanced Baseline Imager (ABI; Schmit et al. 2005) scheduled for launch on the GOES-R series of satellites beginning in 2012.

*Acknowledgments.* The authors would like to express their thanks to several individuals for their contributions to the paper. Mr. Paul Meyer (NASA) provided valuable help with the accessing of the NLCD database and in the production of the tornado track shape files. Mr. Todd Berendes (UAH) provided data processing assistance with the EOS data. Mr. Jason Burks (NWS HUN) was instrumental in getting the initial MODIS and ASTER data into AWIPS and Mr. Chris Darden (NWS HUN) provided insight into the preparation of tornado damage surveys by the NWS. The authors would also like to thank the anonymous reviewers for their thorough review of the manuscript. Their comments and suggestions have led to a substantially improved version of the paper. This research was funded by the NASA Science Mission Directorate's Earth–Sun System Division in support of the Short-term Prediction and Research Transition (SPoRT) program at Marshall Space Flight Center.

## REFERENCES

AIR Worldwide Corporation, 2002: Real-time loss estimates for thunderstorm damage: The event of April 27–28, 2002. AIR Tech. Doc. LPSR 0207, AIR Worldwide Corporation, Boston, MA, 8 pp. [Available online at http://www.air-worldwide.com/_public/NewsData/000259/LaPlata_Tornado_Special_Report.pdf.]

Bentley, M. L., T. L. Mote, and P. Thebpanya, 2002: Using Landsat to identify thunderstorm damage in agricultural regions. *Bull. Amer. Meteor. Soc.,* **83,** 363–376.

Brooks, H. E., and C. A. Doswell III, 2001: Normalized damage from major tornadoes in the United States: 1890–1999. *Wea. Forecasting,* **16,** 168–176.

——, and ——, 2002: Deaths in the 3 May 1999 Oklahoma City tornadoes from a historical perspective. *Wea. Forecasting,* **17,** 354–361.

Bryant, R. B., M. S. Moran, S. A. McElroy, C. D. Holifield, K. J. Thome, T. Miura, and S. F. Biggar, 2003: Data continuity of Earth Observing-1 (EO-1) Advanced Land Imager (ALI) and Landsat TM and ETM+. *IEEE Trans. Geosci. Remote Sens.,* **41,** 1204–1214.

DOC, 2002: NOAA/NWS service assessment: La Plata, Maryland, tornado outbreak April 28, 2002. NOAA/NWS, Dept. of Commerce, Silver Springs, MD. [Available online at ftp://ftp.nws.noaa.gov/om/assessments/laplata.pdf.]

Dyer, R. C., 1988: Remote sensing identification of tornado tracks in Argentina, Brazil, and Paraguay. *Photogramm. Eng. Remote Sens.,* **54,** 1429–1435.

Friday, E., 1994: The modernization and associated restructuring of the National Weather Service: An overview. *Bull. Amer. Meteor. Soc.,* **75,** 43–52.

Fujita, T. T., 1981: Tornadoes and downbursts in the context of generalized planetary scales. *J. Atmos. Sci.,* **38,** 1511–1534.

——, 1987: U.S. tornadoes. Part 1: 70-year statistics. Satellite and Mesometeorology Research Project (SMRP) Research Paper 218, University of Chicago, 122 pp.

Goodman, S. J., W. M. Lapenta, G. J. Jedlovec, J. C. Dodge, and T. Bradshaw, 2004: The NASA Short-term Prediction Research and Transition (SPoRT) Center: A collaborative model for accelerating research into operations. Preprints, *20th Conf. on Interactive Information Processing Systems (IIPS)*, Seattle, WA, Amer. Meteor. Soc., CD-ROM, P1.34.

Henebry, G. M., and I. C. Ratcliffe, 2003: Occurrence and persistence of hailstreaks in the vegetated land surface, Preprints, *17th Conf. on Hydrology*, Long Beach, CA, Amer. Meteor. Soc, CD-ROM, JP5.3.

Homer, C., C. Huang, L. Yang, B. Wylie, and M. Coan, 2004: Development of a 2001 National Landcover Database for the United States. *Photogramm. Eng. Remote Sens.,* **70,** 829–840.

Klimowski, B. A., M. R. Hjelmfelt, M. J. Bunkers, D. Sedlacek, and L. R. Johnson, 1998: Hailstorm damage observed from the *GOES-8* satellite: The 5–6 July 1996 Butte–Meade storm. *Mon. Wea. Rev.,* **126,** 831–834.

Lazzara, M. A., and Coauthors, 1999: The Man computer Interactive Data Access System: 25 years of interactive processing. *Bull. Amer. Meteor. Soc.,* **80,** 271–284.

Levine, M. D., and S. I. Shaheen, 1978: A modular computer vision system for picture segmentation and interpretation. *IEEE Trans. Pattern Anal. Mach. Intell.,* **3,** 540–556.

Missouri Department of Conservation, cited 2005: Missouri forest health highlights 2002. [Available online at http://stlouis.missouri.org/forestkeepers/contactus.html.]

Nair, U. S., J. A. Rushing, R. Ramachandran, K. S. Kuo, R. M. Welch, and S. J. Graves, 1999: Detection of cumulus cloud fields in satellite imagery. *Proc. SPIE,* **3740,** 345–355.

NASA, cited 2005: EO natural hazards: Tornado hits La Plata, Maryland. [Available online at http://earthobservatory.nasa.gov/NaturalHazards/natural_hazards_v2.php3?img_id=3621.]

NCDC, cited 2005: Storm events. [Available online at http://www4.ncdc.noaa.gov/cgi-win/wwcgi.dll?wwEvent~Storms.]

Nelson, C. S., and J. D. Cunningham, 2002: The National Polar-Orbiting Operational Environmental Satellite System future U.S. environmental observing system. Preprints, *Sixth Symp. on Integrated Observing Systems*, Orlando, FL, Amer. Meteor. Soc., CD-ROM, 3.1.

NWS, cited 2005: Butler County tornado map. [Available online at http://www.crh.noaa.gov/pah/storm/butler/map.shtml.]

Parker, M. D., I. C. Ratcliffe, and G. M. Henebry, 2005: The July 2003 Dakota hailswaths: Creation, characteristics, and possible impacts. *Mon. Wea. Rev.,* **133,** 1241–1260.

Schmit, T. J., M. M. Gunshor, W. P. Menzel, J. J. Gurka, J. Li, and A. S. Bachmeier, 2005: Introducing the next-generation Advanced Baseline Imager on GOES-R. *Bull. Amer. Meteor. Soc.,* **86,** 1079–1096.

Schueler, C. F., 2003: NPOESS VIIRS: Next-generation polar-orbiting atmospheric imager. *Proc. SPIE,* **4891,** 50–64.

Segele, Z. T., D. J. Stensrud, I. C. Ratcliffe, and G. M. Henebry, 2005: Influence of a hail streak on boundary layer evolution. *Mon. Wea. Rev.,* **133,** 942–960.

Seguin, W. R., 2002: AWIPS—An end-to-end look. Preprints, *Interactive Symp. on the Advanced Weather Interactive Processing System (AWIPS),* Orlando, FL, Amer. Meteor. Soc., J47–J50.

Speheger, D. A., C. A. Doswell III, and G. J. Stumpf, 2002: The tornadoes of 3 May 1999: Event verification in central Oklahoma and related issues. *Wea. Forecasting,* **17,** 362–381.

StormCenter Communications, cited 2005: Envirocast media update for Thursday, April 1, 2004. StormCenter Communications, Ellicott City, MD. [Available online at http://www.stormcenter.com/media/040401/.]

Strong, C. A., and S. M. Zubrick, 2004: Overview and synoptic assessment of the 28 April 2002 La Plata, MD tornado. Preprints, *22d Conf. on Severe Local Storms*, Hyannis, MA, Amer. Meteor. Soc., CD-ROM, P12.5.

Stumpf, G. J., T. M. Smith, and C. Thomas, 2003: The National Severe Storms Laboratory's contribution to severe weather warning improvement: Multiple-sensor severe weather applications. *Atmos. Res.,* **67-68,** 657–669.

USGS, cited 2005: Tornado samples. [Available online at http://eo1.usgs.gov/tornadosamples.php.]

Vogelmann, J. E., S. M. Howard, L. Yang, C. R. Larson, B. K. Wylie, and N. van Driel, 2001: Completion of the 1990s National Land Cover Dataset for the conterminous United States from Landsat Thematic Mapper data and ancillary sources. *Photogramm. Eng. Remote Sens.,* **67,** 650–661.

Yuan, M., M. Dickens-Micozzi, and M. A. Magsig, 2002: Analysis of tornado damage tracks from the 3 May tornado outbreak using multispectral satellite imagery. *Wea. Forecasting,* **17,** 382–398.